JOURNAL OF MATERIALS SCIENCE 23 (1988) 2613–2621

Characterization of amorphous alloys by thermal analysis techniques

T. J. TAYLOR, Y. P. KHANNA
Corporate Technology, Allied-Signal Inc., Morristown, New Jersey 07960, USA
H. H. LIEBERMANN
Metglas Products, Allied-Signal Inc., Parsippany, New Jersey 07054, USA

Various thermal analysis studies were conducted to characterize metallic glasses. The methods used, namely differential scanning calorimetry, dilatometry, dynamic mechanical analysis and thermomagnetometry, are shown to be useful for studying thermally induced phenomena. Examples covered demonstrate the usefulness of thermal techniques in evaluating structural relaxation, Curie temperature, glass transition, and devitrification processes. A basis of understanding structural relaxation and the glass transition is discussed in terms of a diagram of enthalpy against temperature.

1. Introduction

Rapid solidification from the melt is a technique used to produce alloys of significantly different properties than would be achievable using conventional casting methods. Solidification velocities during conventional casting are sufficiently slow for an alloy to take on ordered, crystalline structures of high thermodynamic stability. In contrast to this, atoms may form metastable crystalline states of low thermodynamic stability, or even totally amorphous states, if the molten alloy is quenched very rapidly (i.e. $> 10^6$ K sec^{-1}). Such rapidly solidified alloys are of great interest and have a number of unique properties which are advantageously used in many applications.

Amorphous alloys, also known as metallic glasses, contain quenched-in excess free volume which plays an important role in the variation of many of the observed properties as it is reduced and redistributed during annealing. This so-called structural relaxation, together with other properties unique to amorphous materials, e.g. glass transition and crystallization phenomena, have been extensively studied by thermal/mechanical techniques at Allied-Signal Inc. At higher temperatures, metastable materials tend to break down and transform to more stable structural forms, the process of which is readily followed using thermal techniques.

A property of ferromagnetic amorphous alloys is the Curie temperature, although it is not unique to this class of materials. The aim of this report is to summarize the various types of thermal/mechanical studies that have been carried out at Allied on amorphous alloys and to demonstrate their utility.

2. Experimental procedure

Differential scanning calorimetry (DSC) scans were obtained with a DuPont 1090 DSC unit using a heating rate of 20 K min^{-1}, argon atmosphere, and gold sample pans. Specific heat (C_p) data were measured using a Perkin-Elmer Model DSC-2C fitted with the TADS data station. Approximately 30 mg of alloy were heated in a crimped aluminium pan at a rate of 10 K min^{-1} in flowing argon.

The thermal expansion studies were conducted using a Netzsch Dilatometer Model 402ES/3 (West Germany), operating in helium and using a 5 K min^{-1} programmed rate. Short lengths of the ribbon were cut and rolled into cylinders (about 1.7 cm long × 3.5 mm in diameter). The cylinders were constrained in an alumina ring, the expansion being measured along the cylinder axis.

Dynamic mechanical analysis data were obtained using a Polymer Laboratories (UK) DMTA unit, which operates in the bending mode of deformation with a fixed frequency and strain value. The frequency at which measurements were made was 1 Hz with a heating rate of 5 K min^{-1}. The sample was mounted as four layers, clamped tightly.

A Perkin-Elmer TGS-2 thermogravimetric analyser (TGA) was used for Curie-point determination by observing the force exerted due to a small permanent magnet positioned below the sample in the instrument. An inert atmosphere of argon was used.

3. Results and discussion

3.1. Structural relaxation

Structural relaxation phenomena are extremely difficult to observe by direct techniques, but result in both major and minor changes in many physical properties of amorphous materials and thus can be studied indirectly [1]. A number of studies of these effects are detailed below.

DSC data were obtained for samples of Metglas* alloy 2605S-2 (nominal composition $Fe_{78}B_{13}Si_9$) which had been annealed for varying lengths of time

*Metglas is a registered trademark of Allied Corporation.

0022–2461/88 $03.00 + .12

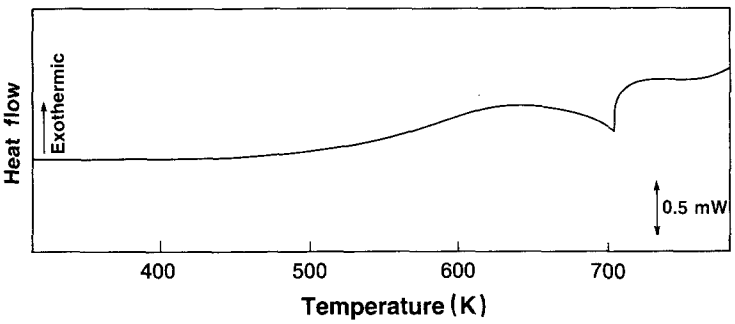

Figure 1 DSC trace of as-cast Metglas alloy 2605S-2 (nominal composition $Fe_{78}B_{13}Si_9$).

at several temperatures [2]. While the purpose of this work was to evaluate resultant changes in the Curie point, the data also gave a qualitative picture of the amount of structural relaxation occurring during annealing. The DSC trace for the as-cast alloy between 320 and 580 K is shown in Fig. 1. Although such qualitative DSC work is not a preferred technique to study subtle thermal events, quantitative DSC (e.g. C_p against temperature) has been carried out previously [3] to support our observations. As can be seen in Fig. 1, two main features are indicated: a very broad exotherm from about 463 to 753 K and a sharp endotherm centred at 685 K. The latter is associated with the Curie point and will be described later.

The exotherm is due to structural relaxation and can be better understood by considering an idealized plot of enthalpy against temperature for an amorphous but crystallizable system (e.g. metallic glasses), as depicted in Fig. 2. As a liquid is very rapidly cooled through its melting point (T_m) the enthalpy of the supercooled liquid continues to fall off, although at a slower rate than if it had crystallized. Although the liquid at temperatures below T_m is metastable with respect to the crystalline state, it is in internal equilibrium, the atomic configuration changing with temperature. This continues until the energy available has lowered to a point where no further rearrangement can occur and the supercooled liquid approaches an isoconfigurational state. The enthalpy then falls much more slowly. A more rapidly quenched liquid will go through this point (the glass transition, T_g) sooner, e.g. following Line 1, whereas a more slowly quenched liquid would, theoretically, follow Line 2. The relaxation process, represented by the dashed line (a) in Fig. 2, is irreversible. This type of relaxation occurs on annealing below T_g and is initially rapid but slows down progressively. Thus a glass relaxes toward equilibrium but is far from achieving it. Such relaxation gives rise to changes such as increases in density, Young's modulus and viscosity, and decreases in enthalpy, diffusivity, internal friction and ductility [4].

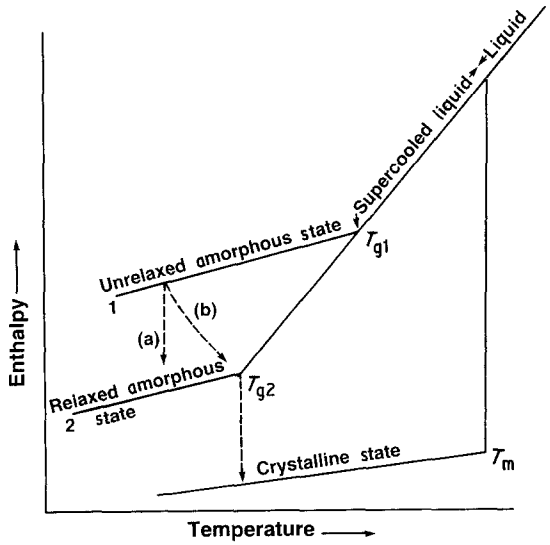

Figure 2 Temperature dependence of enthalpy in an amorphous but crystallizable system. (a) Relaxation during sub-T_g annealing; (b) relaxation during DSC analysis.

Relaxation results in an exothermic peak on DSC scanning, as shown in Fig. 1, and in a shift in the Curie temperature [5, 6]. On plotting the annealing temperatures against time, a series of Curie temperature contour lines is obtained (Fig. 3). These are incomplete but compare well with published data for Metglas alloy 2605 (nominal composition $Fe_{80}B_{20}$) [6]. The latter data show that, at annealing temperatures above 678 K, the Curie point changes very little with increasing annealing time. This kind of diagram is useful in extrapolating relaxation data to lower temperatures to see if relaxation processes are likely to be significant under alloy service conditions. When the T_c levels off on annealing, as shown by Liebermann *et al.* [5] and by Greer [6], it can be presumed that the glass is closer to internal equilibrium. In-depth studies by Greer and Leake [7] have found that the same value of T_c can be obtained after only a short anneal when the starting glass is not in equilibrium, and after a longer anneal when the glass is closer to equilibrium. However, the value departs appreciably during moderate anneals.

A typical plot of expansion during heating and cooling of Metglas 2605S-2 ribbon as a function of temperature up to approximately 700 K is shown in Fig. 4. The alloy undergoes an overall expansion on heating, with a small anomaly occurring near the Curie temperature, at about 690 K. The latter is due to the spontaneous volume magnetostriction of the alloy [8, 9]. The plot shows an initial linear relationship up to about 440 K, followed by a decrease in the slope of the curve. This is the result of an increase in density which, when superimposed on the overall thermal expansion, amounts to about 0.32%. Such a magnitude is in keeping with length-change measurements of some preannealed amorphous alloys [5].

The thermal expansion data shown in Fig. 5 are for a sample which was first annealed at 673 K for 2 h in an 800 A m^{-1} longitudinal field prior to measurement. The expansion was fairly linear up to about 570 K. A reduction in the slope is observed at this point due to

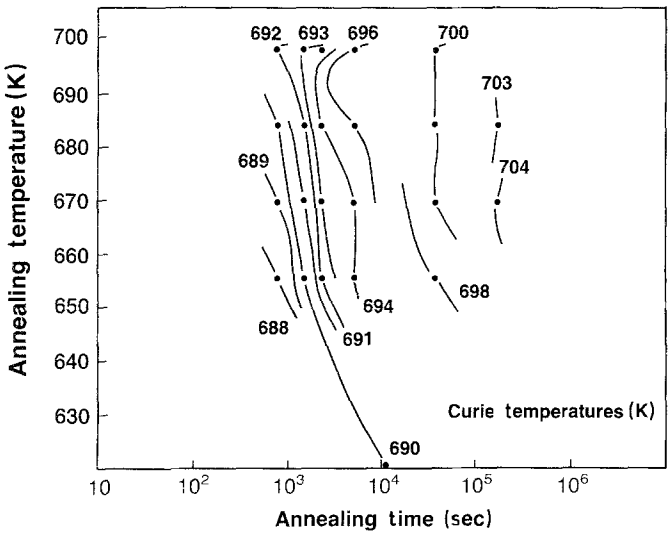

Figure 3 Plot of annealing temperatures against time to indicate Curie temperature contour lines.

spontaneous volume magnetostriction. The slope was less than that observed for the as-cast ribbon. On cooling, the contraction curve retraces the expansion curve, unlike the trace for the as-cast material. Thus, it is clear that the as-cast ribbon structurally relaxes on heating, beginning at 440 K, as is supported by the DSC data.

Dilatometry monitors the reduction or annealing-out of the free volume frozen in during quenching (topological relaxation), but there may also be chemical short-range ordering [10] during structural relaxation. This can be ascribed to a short-range clustering or orientation of atoms and cannot be readily detected. A technique which promises to be extremely sensitive to relaxation phenomena in metallic glasses is dynamic mechanical analysis (DMA). This may enable both topological and compositional structural relaxation to be differentiated as has been discussed by Berry [11]. A plot of the storage modulus (log E') and the damping factor (tan δ) against temperature for a preliminary study of Metglas MBF 2005 brazing foil (nominal composition $Cu_{78}Ni_6P_7Sn_9$) is shown in Fig. 6. While the corresponding DSC trace shown in Fig. 7 illustrates the crystallization exotherm, it is not sensitive to relaxation behaviour. The DMA trace (Fig. 6), on the other hand, clearly illustrates the increase in modulus of the material with increasing ordering, beginning at about 373 K. This gradual modulus increase is followed by a reduction in modulus (and a corresponding tan δ peak) at 472 K due to the sample passing through the glass transition of the alloy.

3.2. Curie temperature

In addition to the use of Curie-temperature studies as a means to observe structural relaxation, the phenomenon is of interest in its own right. When a ferromagnetic object is placed in a magnetic field gradient, it becomes magnetized and a force is exerted on it. The intensity of magnetization is indicated by the strength of this force and is determined by the magnetic field gradient and the magnetic susceptibility of the material. Paramagnetic materials have a small magnetic susceptibility whereas ferromagnetic materials have a large susceptibility. This means that the Curie point can readily be determined using a balance with the sample in a magnetic field gradient and scanning temperature (thermomagnetometry) [12]. The apparent sample weight is dependent on the magnetic susceptibility and gives rise to a perceived weight loss on crossing the Curie temperature, as indicated in Fig. 8. This technique, based on thermogravimetric analysis, has a number of advantages over two other commonly used methods, DSC and permeability measurements. DSC

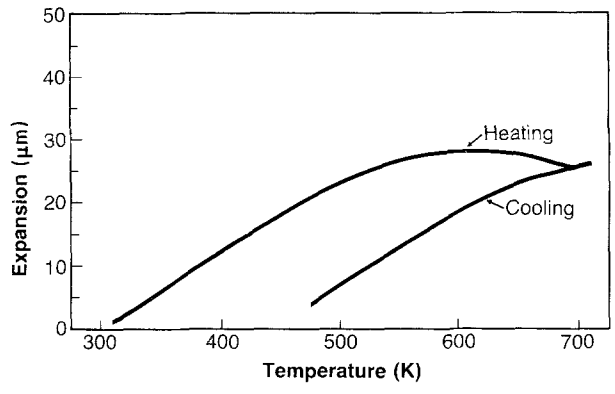

Figure 4 A typical plot of extension during heating and cooling of 2.54 cm wide Metglas 2605S-2 ribbon.

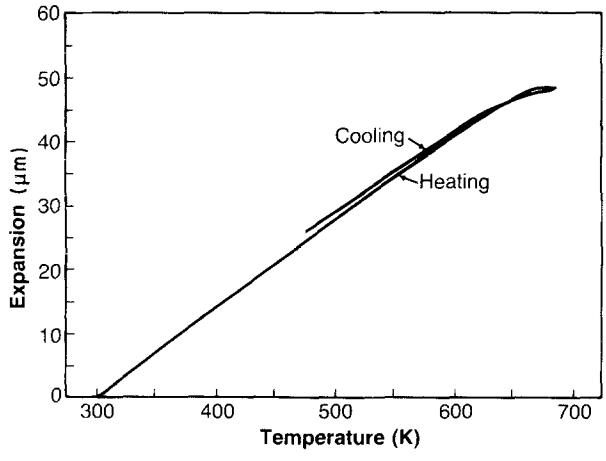

Figure 5 Thermal expansion of Metglas 2605S-2 ribbon after annealing at 673 K for 2 h in an 800 A m^{-1} longitudinal field.

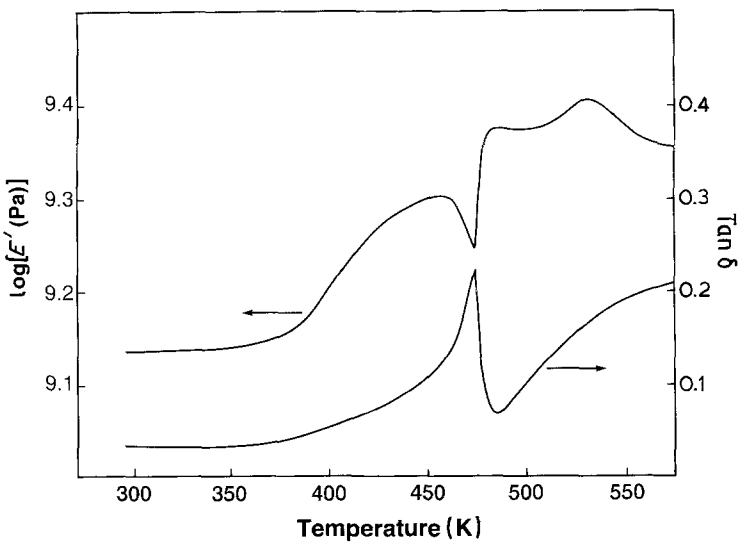

Figure 6 DMA plot of log E' and tan δ against temperature for Metglas brazing foil MBF 2005 (nominal composition $Cu_{78}Ni_6P_7Sn_9$).

relies on the principle that the disappearance of spontaneous magnetization in the vicinity of the Curie temperature is accompanied by changes in the sample's internal energy. These changes can result in an endothermic anomaly in the plot of specific heat against temperature of the type shown in Fig. 1 for Metglas 2605S-2 alloy. However, in some alloys, e.g. Metglas alloy 2605CO (nominal composition $Fe_{66}Co_{18}B_{15}Si_1$), this magnetic transition involves a very small enthalpy change which is difficult to detect. The permeability measurements, although straightforward, use more complex equipment and have longer analysis times than thermal methods. The advantage of the thermomagnetometry technique is that it can be very sensitive and is straightforward and relatively simple to use.

A typical thermomagnetometry trace for an amorphous alloy of nominal composition $Fe_{78}B_{17}Si_5$ is shown in Fig. 9, and shows a Curie temperature of about 691 K. This is followed by a paramagnetic to ferromagnetic transition, indicated by an apparent weight gain, beginning at about 788 K as the material crystallizes. An inflection point in the peak shows that this is a two-stage process. At higher temperatures ferromagnetic to paramagnetic transitions are apparent, corresponding to Curie points for the crystalline phases.

More complicated behaviour has been observed in the case of Metglas alloy 2605CO [13]. The measurement of the Curie point of this alloy presents a difficulty, since the crystallization of the amorphous state begins in the same temperature range as that in which the magnetic transition takes place. This results in two overlapping processes: the loss of ferromagnetism by the amorphous phase and the formation of a ferromagnetic crystalline phase. The latter, in turn, is complex since the initial crystalline phase is metastable and rapidly decays into two more stable phases. Thus, any measured ferromagnetic to paramagnetic transition is not a single event. The situation can be clarified by using very fast heating rates (up to 200 K min^{-1}) to increase the temperature at which crystallization begins, and so enable the initial amorphous phase to be studied. Preliminary experiments with a Nicoseal alloy standard with T_c = 711 K showed that instrumental effects due to differences in heating rates of an order of magnitude (20 to 200 K min^{-1}) give a variation of 4 K in T_c. Fig. 10 shows the thermomagnetometry scans obtained using several heating rates for Metglas alloy 2605CO. At the slowest heating rate of 20 K min^{-1} the Curie temperature cannot be clearly identified since the amorphous phase begins to crystallize as ferromagnetism decays (confirmed by DSC). The inflection at about 708 K

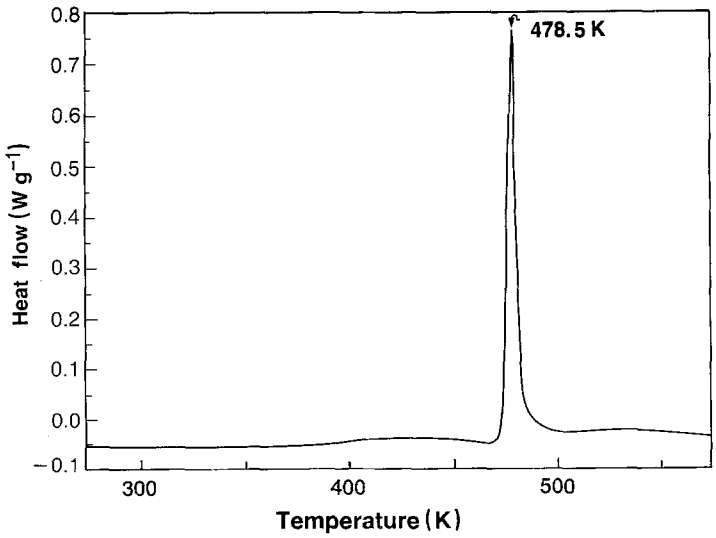

Figure 7 DSC trace for Metglas brazing foil MBF 2005 (nominal composition $Cu_{78}Ni_6P_7Sn_9$).

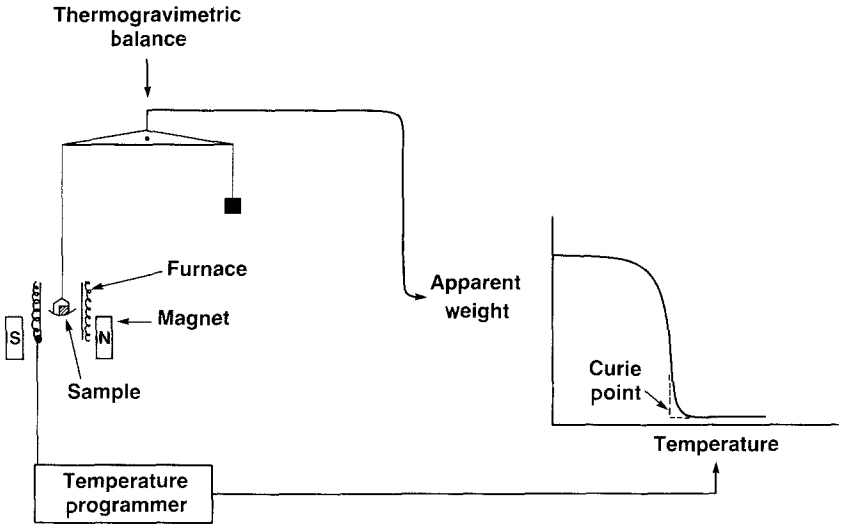

Figure 8 Schematic diagram of the instrumental set-up for measuring Curie temperatures by thermomagnetometry.

has been reported as the Curie temperature [14]. However, by raising the heating rate the crystallization process can be delayed to higher temperatures and the true Curie transition of the amorphous phase can be observed. Thus, the trace obtained at 200 K min^{-1} enables the curve due to loss of ferromagnetism to be extrapolated, giving a hypothetical Curie temperature of around 840 K.

3.3. Glass transition

As indicated by Fig. 2, a liquid supercooled below the equilibrium crystallization temperature for that composition initially follows so-called ideal equilibrium cooling. The material is of course, in a non-equilibrium state relative to the crystalline state. Atomic motion becomes more restricted with continued cooling and the local "structure" (volume in which each atom resides) plus a smaller excess volume gets continually redistributed and reduced. This process is both time- and temperature-dependent. Ultimately a point is reached at which the cooling rate is too fast for further redistribution and reduction so that the structure "locks in" and forms a glass. Reheating at the same (infinite) rate along the cooling curve (Line 1 in Fig. 2) would ideally result in the reverse process occurring, i.e. short-range diffusional motion would again be possible at T_{g1}. Sub-T_g annealing, either isothermally (Process (a) in Fig. 2), or by heating at a rate significantly slower than the initial cooling rate, such as during a DSC scan (Process (b) in Fig. 2), results in a lowering of the free energy and excess volume of the material, allowing it to more closely approach the ideal equilibrium cooling line. Thus, the T_g observed in a DSC experiment will be lower than the temperature at which the molten metal became glassy during production. It is quite likely that the observed T_g using DSC is close to that of the fully relaxed glass. It should be noted that the topological changes associated with annealing and with cooling along the equilibrium cooling line do not necessarily imply the occurrence of any chemical interactions.

In addition to the time/temperature effects on T_g there is clearly a dependence on the composition of the

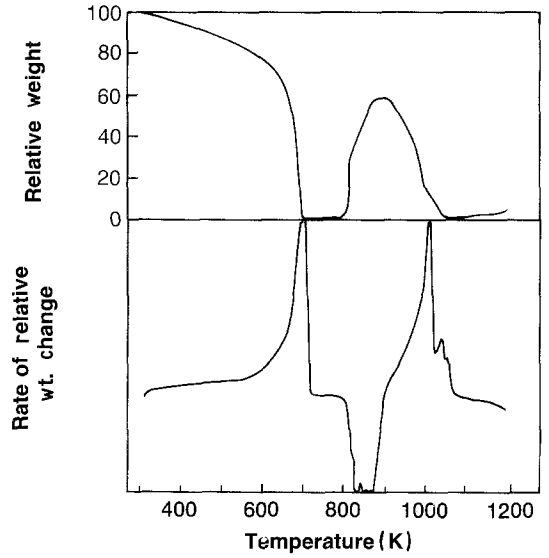

Figure 9 Thermomagnetometry scan of amorphous $Fe_{78}B_{17}Si_5$.

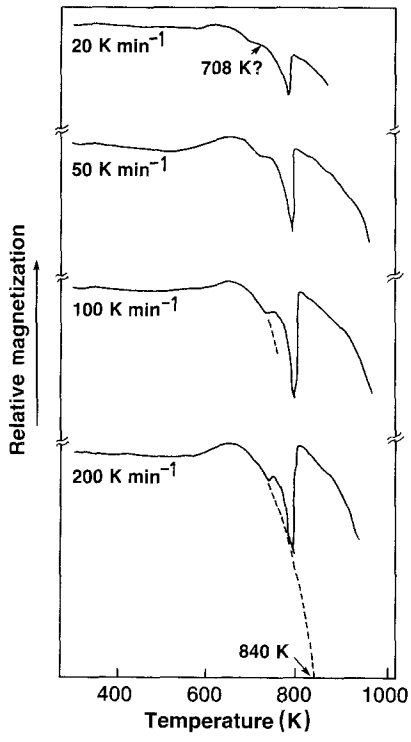

Figure 10 Thermomagnetometry data for Metglas alloy 2605CO (nominal composition $Fe_{66}Co_{18}B_{15}Si_1$) using various heating rates.

material. In an ideal situation, involving no short-range interactions in the molten or supercooled state, the amorphous metal can be considered to be a mixture of hard spheres. Various studies, e.g. Chen *et al.* [15], have attempted to show that partial substitution of an element possessing a larger ionic radius for a component of smaller radius will lower the T_g. This is explained in terms of increasing excess volume, occurring with a mixture of hard spheres of differing radii compared with a uniform hard-sphere assembly, which promotes short-range diffusional motion. However, the data are not unequivocal and studies here have shown an opposite effect. For example [16], substituting molybdenum (metallic radius 0.136 nm) for iron (metallic radius 0.124 nm) in the metallic glass $Fe_{67}Cr_7Ni_5Co_3B_{18}$ results in an increasing T_g (Table I). This can be explained if the increased mass of molybdenum over iron (i.e. 96 compared with 56) increases the energy needed for diffusional motion. Moreover, most metallic glasses cannot be regarded as purely random mixtures of hard spheres. Short-range chemical interactions, e.g. between metallic and non-metallic elements, may "stiffen" the material and raise the T_g. Thus any study of the glass transition of metallic glasses should attempt to elucidate the nature of these interactions and define any local "structure".

Various studies (e.g. Greer *et al.* [17], and Komatsu and Matusita [18]) have suggested that the glass may undergo reversible relaxations during annealing, and achieve quasi-equilibrium states between the heating lines (Lines 1 and 2) in Fig. 2. In addition, it has been claimed [19] that a glass may be heated and thereby displaced from its ideal equilibrium line towards the crystalline enthalpy line while remaining amorphous. These processes are not readily explained using the concepts of structural relaxation discussed so far. However, as these concepts have been successfully applied to many types of amorphous material it is reasonable that metallic glasses ought to exhibit some characteristics basic to all glasses. So-called short-range or chemical ordering may involve reversible changes which would not directly involve changes in overall "structure" or atomic topology (and thus T_g) changes. For example Komatsu and Matusita [18] consider the possibility of $(Ni_{0.75}Fe_{0.25})_3(Si,B)$ trigonal prisms existing in $Fe_{15}Ni_{63}Si_8B_{14}$ metallic glass. On heating, a temperature is reached at which changes occur in various properties which are ascribed as being due to movements of iron and nickel within the trigonal prism. This is separate from the longer-range atom motions which are related to T_g but do not necessarily influence T_g. Also, this type of motion is known to affect the Curie temperature and a series of such motions could give the appearance of local equilibrium points on Fig. 2 between Lines 1 and 2 of the type observed by Greer and Leake [7].

TABLE I Variation of the glass transition temperature with composition for $Fe_{67-x}Mo_xCr_7Ni_5Co_3B_{18}$

x	T_g (K)
0	715
4	765
8	786
12	805

3.4. Devitrification

The properties of metallic glasses obviously depend on their amorphous nature which, as previously discussed, depends on the thermal treatment to which these materials are subjected. For example, in order to obtain optimal magnetic properties, the magnetic glasses have to be annealed below the crystallization temperature, often in the presence of a magnetic field. Since the properties begin to deteriorate with the onset of crystallization, the time–temperature dependence of crystallization is important in defining the proper annealing processes. An example of the application of thermal analysis is in the study of the crystallization kinetics of Metglas alloys by isothermal DSC measurements [20]. The study utilized an Arrhenius-type equation, representing the onset of crystallization:

$$t = t_0 \exp(E/RT)$$

where t is the time required for the onset of crystallization, t_0 a constant and T the isothermal annealing temperature. Three different alloy compositions were studied by isothermal DSC and log t plotted against $1/T$ (Fig. 11). From the plots a linear equation can be generated enabling short-term time–temperature data to be calculated for the annealing processes (Tables II to IV).

A study of the formation and magnetic properties of Fe–B–Si metallic glasses has been reported in the literature [21, 22]. Thermal stability (devitrification

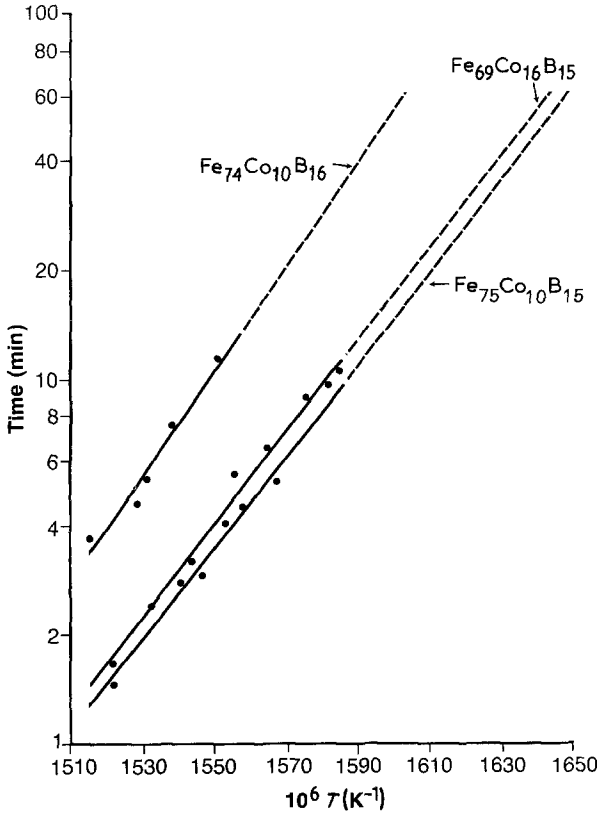

Figure 11 Crystallization onset time against reciprocal annealing temperature for amorphous alloys $Fe_{74}Co_{10}B_{16}$, $Fe_{75}Co_{10}B_{15}$ and $Fe_{69}Co_{16}B_{15}$.

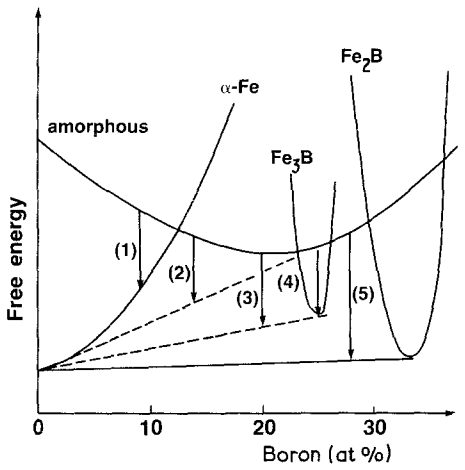

Figure 12 Hypothetical diagram of the free energy for the various phases in Fe–B alloys. (1) Polymorphous crystallization of α-iron; (2) primary crystallization of α-iron; (3) eutectoid crystallization, α-Fe + Fe_3B; (4) polymorphous crystallization of Fe_3B; (5) eutectoid crystallization, α-Fe + Fe_2B.

behaviour) was characterized as a function of composition. In any glassy system, the transition of a metastable amorphous phase into crystalline phases can proceed by any one of three processes [23]. These are best considered by reference to a free-energy diagram for the various phases, for example those possible in an Fe–B system shown in Fig. 12 [23]. The equilibrium common tangent is shown by a solid line and possible metastable equilibria are marked by dashed tangents. Depending on the alloy composition, then, examples of the three possible reaction types are shown in Fig. 13 [23] and are summarized below.

(a) *Polymorphous crystallization*: crystallization without change of concentration across the amorphous/crystalline interface. This metastable phase will then transform into the stable equilibrium phases.

(b) *Primary crystallization*: of one of the primary phases, e.g. α-iron (Process 2 in Fig. 12). During this reaction, the amorphous phase will be enriched in boron until further crystallization is stopped on reaching the metastable equilibrium between α-iron and amorphous Fe–B. This amorphous matrix can transform later or at higher temperatures by one of the mechanisms described here.

(c) *Eutectoid crystallization*: simultaneous crystallization of two or more crystalline phases.

In the study [22] of the devitrification in $Fe_{82}B_{18-x}Si_x$, it was shown that in the case of alloys containing low silicon concentrations (< 2 at %) these transform directly to α-(Fe, Si) (primary crystallization) and Fe_3B (polymorphous crystallization) in a single step. At higher silicon levels, a two-step transformation occurs. These alloys undergo primary crystallization to form α-(Fe, Si) crystallites within the amorphous matrix. At higher temperatures, the remaining glass crystallizes into α-(Fe, Si) and Fe_3B. Compositions within the eutectic trough undergo eutectic crystallization simultaneously, i.e. forming α-(Fe, Si) and Fe_3B. Fe_3B is itself metastable and decomposes into α-Fe and Fe_2B with further heating.

A systematic study of the variation of the crystallization kinetics in Fe–B–Si amorphous alloys has been carried out by Ramanan and Fish [24]. While confirming previously-noted characteristics of these alloys, they used DSC to monitor the kinetics. They used the Johnson–Mehl–Avrami equation,

$$1 - \alpha = \exp(-kt^n)$$

where α is the fraction converted, k is the rate constant, t the time and n the Avrami exponent which has been shown to describe crystallization phenomena. The rate constant is assumed to be governed by an Arrhenius law:

$$k = A \exp(E/RT)$$

where T is the temperature, A is a constant, E is the activation energy and R is the gas constant. Using these equations (see Khanna and Taylor [20] for a fuller discussion of the use of these expressions) the

TABLE II Annealing of amorphous alloy $Fe_{74}Co_{10}B_{16}$

Temperature, T (K)	$1/T$ (K^{-1})	Time, t (min)	log t	Arrhenius plot			Activation energy, ΔE (kJ mol^{-1})
				Slope (K)	Intercept	Equation	
645	0.001550	11.0	1.041				
650	0.001538	7.5	0.875				
653	0.001531	5.5	0.740	1.4245×10^4	−21.05	$\log t = \frac{14245}{T} - 21.05$	273
655	0.001527	4.8	0.681				
660	0.001515	3.6	0.556				

TABLE III Annealing of amorphous alloy $Fe_{75}Co_{10}B_{15}$

Temperature, T (K)	$1/T$ (K^{-1})	Time, t (min)	log t	Arrhenius plot			Activation energy, ΔE (kJ mol^{-1})
				Slope (K)	Intercept	Equation	
635	0.001575	5.5	0.740				
638	0.001567	4.5	0.653				
643	0.001555	3.0	0.477	1.2757×10^4	−19.35	$\log t = \frac{12757}{T} - 19.35$	244
645	0.001550	2.8	0.447				
648	0.001543	2.3	0.362				
653	0.001531	1.5	0.176				

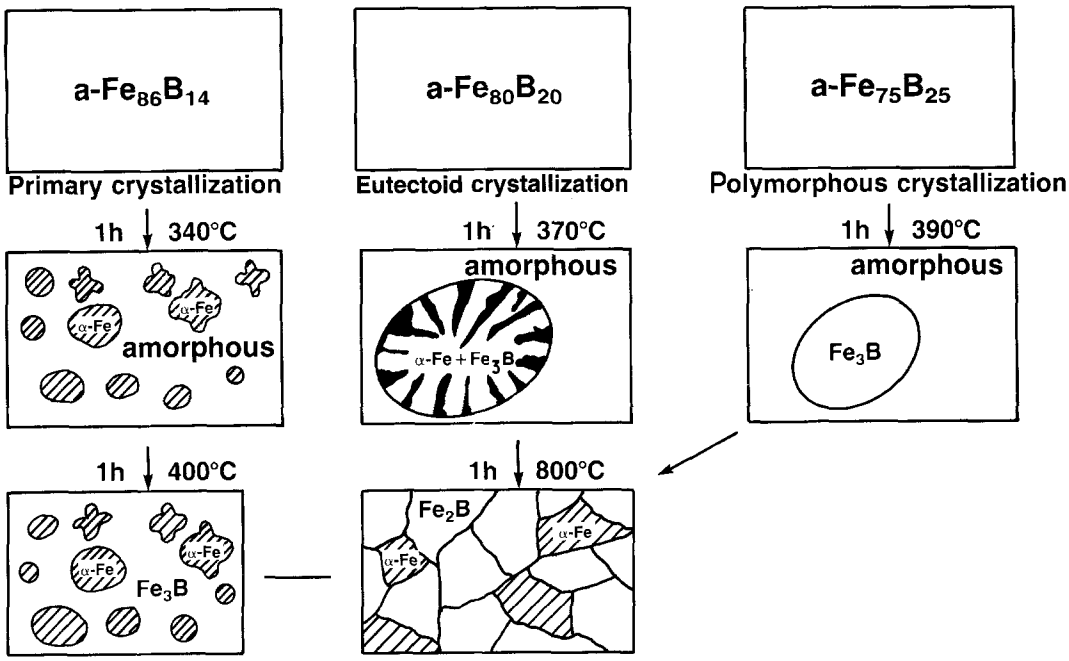

Figure 13 Schematic diagram of typical crystallization reactions in Fe–B alloys.

variation of E and n as a function of composition was studied and is shown [24] in Fig. 14. This indicates that in the hypoeutectoid (i.e. iron-rich) region, E, and thus the thermal stability of the glasses, is fairly independent of the silicon content but decreases very rapidly with increasing iron content. In the hypereutectoid region, however, the effect of silicon is quite dramatic. E rises sharply from 2.5 eV at^{-1} for Fe–B to 4.5 eV at^{-1} with the addition of 3 at % Si, regardless of iron and boron contents. The behaviour of n in the Fe–B–Si system was found to be more complex than that for E. Also, n was more or less constant along the eutectic trough and in most of the hypoeutectoid region; in the hypereutectoid region, the value of n tends slowly towards 3 as the

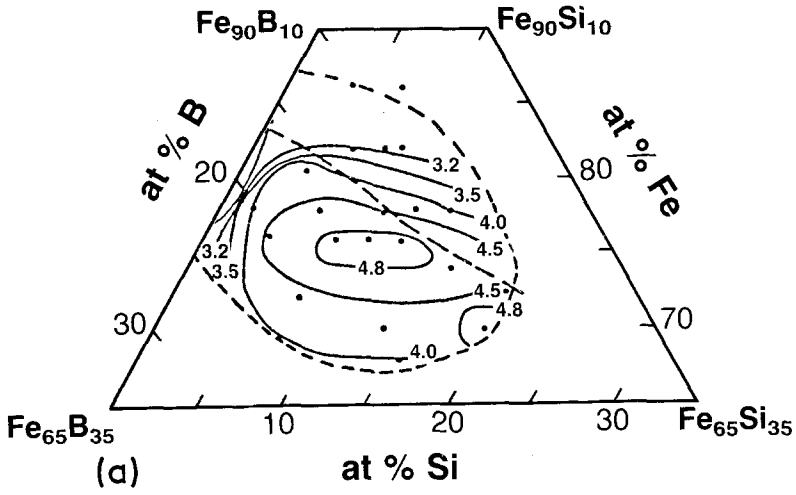

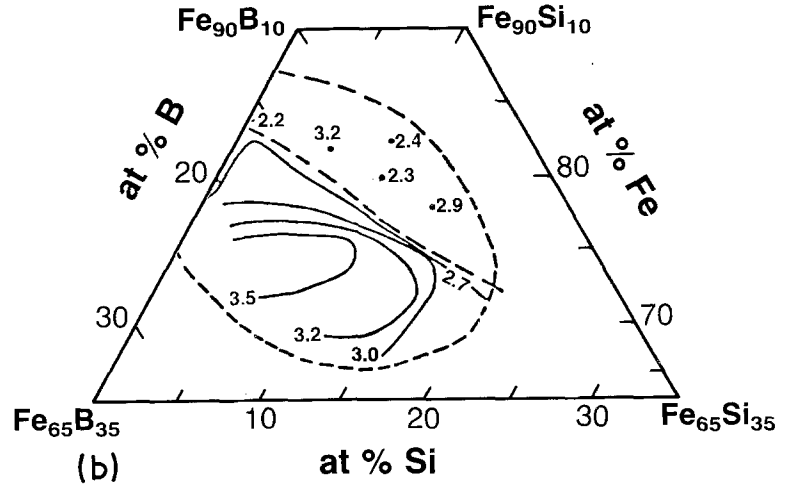

Figure 14 Variation of the crystallization kinetics with composition of Fe–B–Si alloys: (a) E, (b) n.

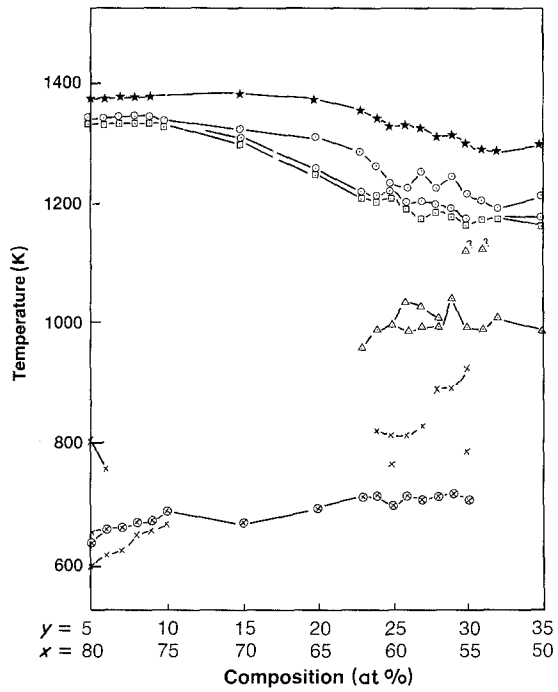

Figure 15 Partial phase diagram for the $Ni_xMn_yB_{15}$ system. (⊗) Main and (x) small devitrification peaks; (△) endothermic solid-state transitions; (⊡) first and (⊙) subsequent solidus temperatures; (★) liquid temperatures.

edge of the glass-forming region is approached, except at around 10 at % Si where it varies rapidly.

In a study to determine the phase equilibria in the ternary Ni–Mn–B system, beginning with amorphous ribbons, the variation of crystallization pattern with composition was noted [2]. This is indicated as part of the phase diagram for the $Ni_xMn_yB_{15}$ system shown in Fig. 15. The types of crystallization occurring are unclear without X-ray analysis, but the phase diagram clearly shows that over a certain composition range (i.e. $Ni_{62-50}Mn_{23-35}B_{15}$) metastable phases are formed which decompose to more stable forms at higher temperatures.

4. Conclusion

The phenomena of solid-state transitions in amorphous but crystallizable metallic alloys, studied by thermal and related techniques in our laboratories, have been reviewed. In particular, four phenomena are explored using these techniques, namely structural relaxation, the Curie transition, the glass transition and devitrification. A diagram of enthalpy against temperature is used to provide the basis of understanding structural relaxation and the glass transition and their dependence on annealing.

References

1. H. S. CHEN, in "Amorphous Metallic Alloys", edited by F. E. Luborsky (Butterworths, Boston, 1983) p. 169.
2. T. J. TAYLOR, unpublished work (1983 to 1986).
3. R. J. J. MARTIS, T. J. TAYLOR and Y. P. KHANNA, *J. Non-Cryst. Solids* **94** (1987) 209.
4. A. L. GREER, *ibid.* **61/62** (1984) 737.
5. H. H. LIEBERMANN, C. D. GRAHAM and P. J. FLANDERS, *IEEE Trans. Magn.* **MAG-13** (1977) 1541.
6. A. L. GREER, *Thermochim. Acta* **42** (1980) 193.
7. A. L. GREER and J. A. LEAKE, *J. Non-Cryst. Solids* **33** (1979) 291.
8. K. FUKAMICHI, in "Amorphous Metallic Alloys", edited by F. E. Luborsky (Butterworths, Boston, 1983) p. 319.
9. R. HASEGAWA, in "Glassy Metals: Magnetic, Chemical and Structural Properties", edited by R. Hasegawa (CRC Press, Boca Raton, Florida, 1983) p. 173.
10. H. S. CHEN, *J. Non-Cryst. Solids* **46** (1981) 289.
11. B. S. BERRY, in "Metallic Glasses", edited by J. J. Gilman and H. J. Leamy (ASM, Metals Park, Ohio, 1978) p. 161.
12. A. NISHIYAMA and R. ISHADA, *Trans. Jpn Inst. Metals* **3** (1962) 185.
13. A. RABINKIN, unpublished work (1985).
14. ALLIED-SIGNAL, Metglas Products Data Sheet for Magnetic Alloys (Parsippany, NJ 07054, USA, 1983).
15. H. S. CHEN, J. T. KRAUSE and E. A. SIGETY, *J. Non-Cryst. Solids* **13** (1973/74) 321.
16. J. J. BELLES, unpublished work (1974).
17. A. L. GREER, M. R. J. GIBBS, J. A. LEAKE and J. E. EVETTS, *J. Non-Cryst. Solids* **38/39** (1980) 379.
18. T. KOMATSU and K. MATUSITA, *J. Mater. Sci.* **21** (1986) 1693.
19. S. M. REKHSON, *J. Non-Cryst. Solids* **84** (1986) 68.
20. Y. P. KHANNA and T. J. TAYLOR, *Polym. Sci. Eng.* **27** (1987) 764.
21. F. E. LUBORSKY, J. J. BECKER, J. L. WALTER and H. H. LIEBERMANN, *IEEE Trans. Magn* **MAG-15** (1979) 1146.
22. N. DECRISTOFARO, A. FREILICH and G. FISH, *J. Mater. Sci.* **17** (1982) 2365.
23. U. HEROLD and U. KOSTER, in "Proceedings of 3rd International Conference on Rapidly Quenched Metals", edited by B. Cantor (Metals Society, London, 1978) p. 281.
24. V. R. V. RAMANAN and G. E. FISH, *J. Appl. Phys.* **53** (1982) 2273.

Received 23 July
and accepted 23 October 1987

TABLE IV Annealing of amorphous alloy $Fe_{69}Co_{16}B_{15}$

Temperature, T (K)	$1/T$ (K^{-1})	Time, t (min)	log t	Arrhenius plot			Activation energy, ΔE (kJ mol^{-1})
				Slope (K)	Intercept	Equation	
627	0.001595	11.00	1.040				
628	0.001592	10.00	1.000				
630	0.001587	9.00	0.954				
635	0.001575	6.40	0.806				
638	0.001567	5.50	0.740	1.3029×10^4	−19.73	$\log t = \frac{13029}{T} - 19.73$	250
640	0.001563	4.10	0.613				
643	0.001555	3.13	0.496				
648	0.001543	2.40	0.380				
653	0.001531	1.65	0.217				